CHEMISTRY OF MATERIALS
Cite This: Chem. Mater. 2018, 30, 4887−4891
Communication
pubs.acs.org/cm

Anion Exchange in Cesium Lead Halide Perovskite Nanocrystals and Thin Films Using Trimethylsilyl Halide Reagents

Sidney E. Creutz, Evan N. Crites, Michael C. De Siena, and Daniel R. Gamelin*

Department of Chemistry, University of Washington, Seattle, Washington 98195-1700, United States

Supporting Information

The excellent optoelectronic properties and facile synthesis of $CsPbX_3$ (X = Cl, Br, I) colloidal nanocrystals have made them the subject of intense scientific interest since they were first reported in 2015.[1,2] One of the most appealing aspects of $CsPbX_3$ nanocrystals, beyond their high luminescence efficiencies, is their widely tunable emission wavelength. By changing the halide composition, the entirety of the visible spectrum can be accessed. Nanocrystals with different halide compositions can be synthesized directly or accessed through postsynthetic anion exchange from a single starting composition.[3,4] Anion-exchange reactivity is not limited to the cesium lead halide perovskites; similar behavior has been observed and exploited in a range of halide-based nanocrystals including hybrid organic−inorganic lead halide perovskites ($MAPbX_3$, MA = $CH_3NH_3^+$), ternary bismuth halides ($MA_3Bi_2X_9$), cesium antimony halides ($Cs_3Sb_2X_9$), and elpasolites (Cs_2AgBiX_6).[5−8] Anion exchange appears to be a ubiquitous and powerful feature of metal-halide nanocrystal chemistry.

Despite the relative ease of anion-exchange reactions in lead halide perovskite nanocrystals, common methods can present complications. The structural lability of halide perovskite nanocrystals is now well-appreciated, and it has been demonstrated that a wide range of reagents, solvents, and surfactants can cause nanocrystal degradation, e.g., conversion to related phases or stoichiometries (Scheme 1). For instance, $CsPbBr_3$ nanocrystals can be converted partially or fully to Cs_4PbBr_6 nanocrystals through treatment with surfactants including an excess of oleylamine.[9] On the other hand, addition of an alkylammonium bromide surfactant causes formation of $CsPb_2Br_5$.[10] Given these results, some of the most commonly used anion-exchange reagents, alkylammonium halides and surfactant-containing metal halide salt solutions, also risk inadvertently causing some degree of decomposition or undesired transformation of halide-based nanocrystals. Moreover, the need to purify samples after anion exchange to remove excess reagents and reaction byproducts can cause further nanocrystal degradation. These issues are exacerbated in materials with more complex compositions beyond $CsPbX_3$, such as doped nanocrystals, where exposure to excess ligands or parent cations can cause undesired dopant loss.[11]

Scheme 1. Anion Exchange Reactions and Related Transformations

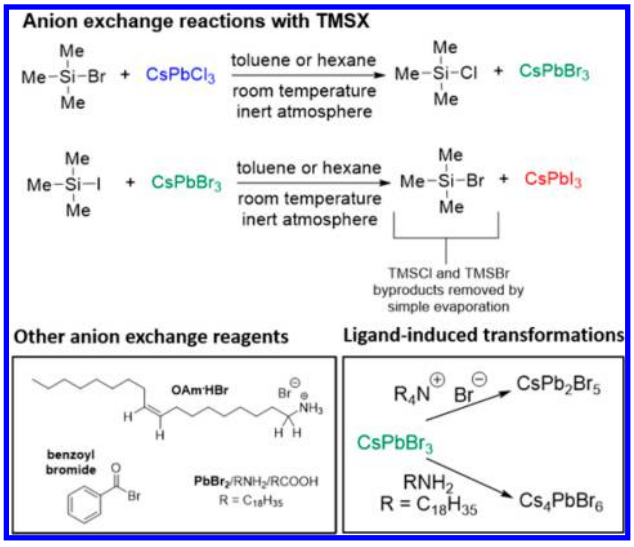

Here, we describe the use of trimethylsilyl halides (TMSX, X = Cl, Br, I) as effective reagents for anion exchange in $CsPbX_3$ nanocrystals. We recently introduced the use of TMSX anion-exchange reagents for halide nanocrystals, specifically elpasolites (double-perovskites).[7] Notably, only TMSBr and TMSI allowed successful synthesis of $Cs_2AgBiBr_6$ and Cs_2AgBiI_6 nanocrystals from their lighter halide congeners, whereas more common anion-exchange reagents caused partial decomposition of the nanocrystals to other phases. We have since found TMSX reagents to be broadly useful in anion-exchange reactions involving a range of metal halide nanocrystals, and their use has generally supplanted other anion-exchange reagents in our laboratory. Although not discussed here, we have also found that TMSX reagents are useful for the direct synthesis of $CsPbCl_3$ and $CsPbBr_3$ nanocrystals (see SI).[12] The results presented here highlight some key advantages of TMSX as nanocrystal anion-exchange reagents. Foremost among these advantages are (*i*) their inertness toward undesired side reactions, (*ii*) their favorable thermodynamics, which allow nearly stoichiometric incorporation of heavier halides into $CsPbX_3$ nanocrystals, and (*iii*) their volatility, which enables nanocrystal purification with no workup other than drying at room temperature (Scheme 1).

TMSCl, TMSBr, and TMSI are all relatively volatile nonpolar liquids with boiling points of 57, 79, and 107 °C, respectively. They are readily miscible with nonpolar alkane and arene solvents such as hexane and toluene. These electrophilic reagents are known for their reactivity with a wide range of nucleophiles; typical reactions involve substitution of the halide for a nucleophile resulting in a

Received: May 17, 2018
Revised: July 12, 2018
Published: July 13, 2018

DOI: 10.1021/acs.chemmater.8b02100
Chem. Mater. 2018, 30, 4887−4891

stronger Si-nucleophile bond, e.g., to generate Si−O or Si−N bonds.[13−15] The Si−X bond strength decreases significantly from the lighter to the heavier halides, with TMS−X bond dissociation energies of 113, 96, and 77 kcal/mol for X = Cl, Br, and I, respectively.[16] These numbers suggest that reactions involving substitution of, e.g., a Si−Cl bond for a Si−Br bond or a Si−Br bond for a Si−I bond, are likely to be favorable.

To test the utility of TMSX anion-exchange reagents with perovskite nanocrystals, we reacted $CsPbX_3$ (X = Cl, Br) nanocrystals with different amounts of TMSX (X = Br, I) in hexane or toluene solutions at room temperature (Scheme 1). The reactions are generally rapid, reaching completion within ∼5 min. Figure 1 shows the results (photoluminescence

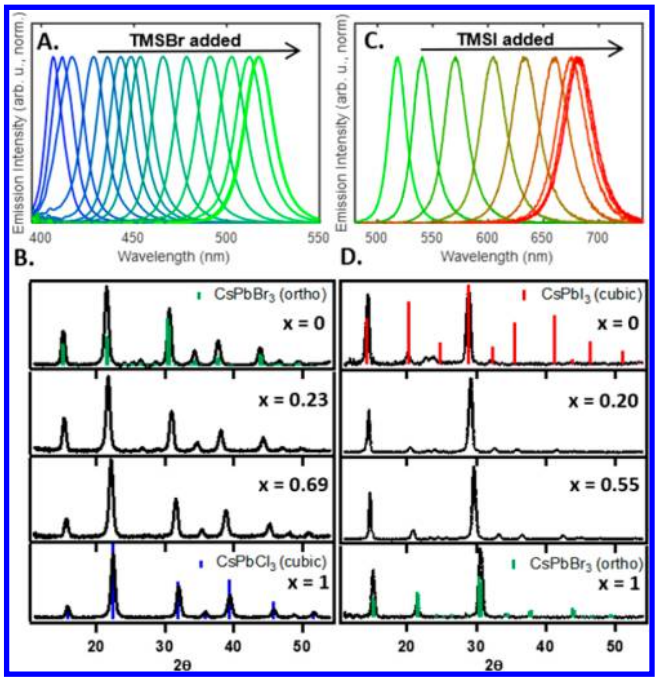

Figure 1. (A, B) Treatment of $CsPbCl_3$ with TMSBr, generating $CsPbCl_{3x}Br_{3(1-x)}$; normalized photoluminescence spectra (A) and selected powder XRD data (B) are shown. (C, D) Treatment of $CsPbBr_3$ with TMSI, generating $CsPbBr_{3x}I_{3(1-x)}$; normalized photoluminescence spectra (C) and selected powder XRD data (D) are shown. Reference patterns for orthorhombic (X = Br) and cubic (X = Cl, I) $CsPbX_3$ are given; values of x are determined using Vegard's law.

spectra and selected powder XRD data) of these exchange reactions as a function of the equivalents of TMSX added to 12 nm $CsPbCl_3$ nanocrystals or 14 nm $CsPbBr_3$ nanocrystals. The emission spectra redshift as x is decreased in $CsPbCl_{3x}Br_{3(1-x)}$ nanocrystals and in $CsPbBr_{3x}I_{3(1-x)}$ nanocrystals, concomitant with increases in the lattice parameters measured by PXRD. Compositions were determined using Vegard's law and confirmed by SEM/EDS for a subset of samples (see SI). Samples treated with TMSX retain good quantum yields, and TEM and XRD analysis illustrate that the general nanocrystal shape and size distribution is preserved during the exchange, with a slight increase in average size (see SI). The XRD of the $CsPbI_3$ nanocrystals, which are not well described by the cubic perovskite phase, will be discussed below. As expected from the strong thermodynamic driving force for exchange to heavier halides, the reactions reach complete conversion with only a slight excess of the heavier TMSX reagent. This result also suggests that the reverse reactions should be highly disfavored; indeed, a large excess of TMSX reagent is required to drive the exchange from Br → Cl or I → Br (see SI).

It is instructive to compare the TMSX reagents to other common anion-exchange reagents used with $CsPbX_3$ nanocrystals. Figure 2B compares Cl-to-Br exchange reactions using

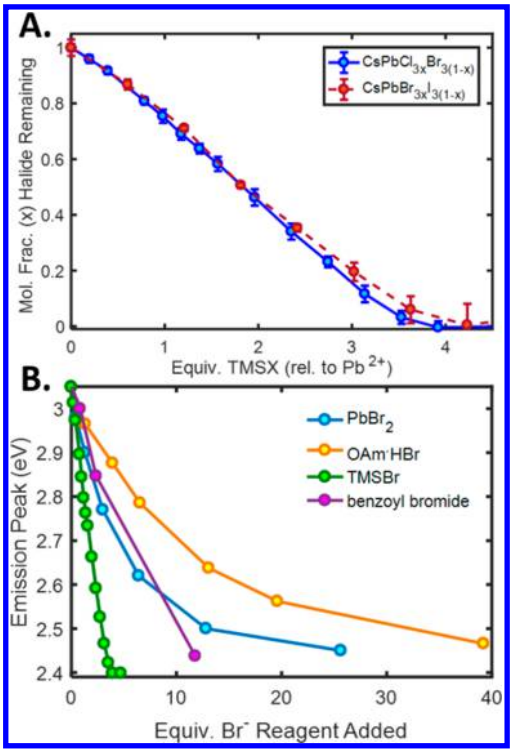

Figure 2. (A) Composition of $CsPbCl_{3x}Br_{3(1-x)}$ (solid blue) and $CsPbBr_{3x}I_{3(1-x)}$ (dashed red) nanocrystals as a function of the equivalents of TMSX reagents (X = Br or I, respectively) added. (B) Comparison of anion exchange reactions from $CsPbCl_3$ to $CsPbCl_{3x}Br_{3(1-x)}$ using different reagents, showing the shift in emission peak as increasing amounts of Br^- reagent are added.

TMSBr, $PbBr_2$, OAm·HBr, and benzoyl bromide[17] by plotting the energy of the emission maximum as a function of added equivalents of Br^- in each case. Compared with TMSX, anion exchange using OAm·HBr requires a large excess of reagent. This result highlights the contrasting thermodynamics of anion exchange with TMSX and reagents such as OAm·HBr; the latter reaction is thermodynamically uphill and hence requires a large excess of reagent to force the equilibrium in favor of bromide incorporation. Using $PbBr_2$, the nanocrystal composition approaches only $\sim CsPbCl_{1.5}Br_{1.5}$ once ∼3 equiv of Br^- have been added. Anion exchange reactions with $PbBr_2$ and OAm·HBr have been examined previously, with results similar to what we observe here.[3,18] We also observed that some of these reagents, particularly OAm·HBr and the $PbBr_2$ solution, sometimes lead to partial decomposition of the nanocrystal products (see SI). In contrast, $CsPbX_3$ nanocrystals remain stable in the presence of extremely large excesses of TMSX, even in pure TMSX, highlighting the inertness of these reagents with respect to undesired side reactions (see SI).

To probe whether the specific reactions described in Scheme 1 are actually operative, we probed the anion-exchange reaction mixtures by ^{1}H NMR. TMS groups have characteristically sharp, upfield ^{1}H NMR resonances that facilitate

DOI: 10.1021/acs.chemmater.8b02100
Chem. Mater. 2018, 30, 4887−4891

identification of TMS-containing species in solution, and TMSCl, TMSBr, and TMSI can be readily distinguished in d_8-toluene (Figure 3). Figure 3A shows the ^{1}H NMR spectrum of a starting sample of 7 nm $CsPbCl_3$ nanocrystals in d_8-toluene; broad resonances characteristic of ligands associated with the nanocrystal surfaces are evident.[19] The relatively downfield shift of the α protons and the peak at ~7.5 ppm attributable to a protonated amine moiety suggest that the associated oleylamine is primarily present as oleylammonium, consistent with evidence from experimental and computational studies suggesting that $CsPbX_3$ nanocrystals are stabilized in solution in large part by ionic interactions between surface halides and alkylammonium cations.[19,20] Upon addition of TMSBr to this sample, a ^{1}H NMR resonance corresponding to TMSCl appears that increases in intensity as more TMSBr is added (Figure 3C), with concomitant changes to the absorption and emission spectra, indicating anion exchange. Significant TMSBr is only observed after anion exchange has reached completion. Only minor amounts of other TMS-containing species are observed. In particular, a resonance is observed at 0.13 ppm that was also detectable in the reference spectrum of pure TMSX and that may be due to reaction with trace water or hydroxide. Other possible side reactions such as with oleates to generate silyl oleates seem to be negligible. Similar behavior is observed by ^{1}H NMR for reaction of $CsPbBr_3$ nanocrystals with TMSI (Figure 3D). These results confirm the reactions illustrated in Scheme 1.

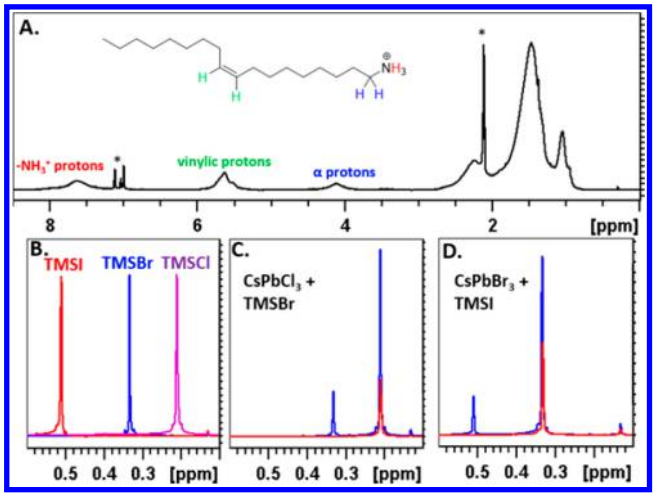

Figure 3. NMR data on $CsPbCl_3$ nanocrystals and on anion exchange reactions. (A) ^{1}H NMR spectrum of initial 7 nm $CsPbCl_3$ nanocrystals in d_8-toluene; Asterisk denotes solvent resonances (C_7HD_7). The vinylic resonance likely includes contributions from both oleylamine and oleate species. (B) ^{1}H NMR spectra of TMSCl, TMSBr, and TMSI. (C, D) ^{1}H NMR spectra of anion exchange reactions treating $CsPbCl_3$ or $CsPbBr_3$ nanocrystals with TMSBr or TMSI, respectively, at partial conversion (red) and after full conversion (blue). See SI for full spectra.

From a practical standpoint, a key advantage of TMSX for nanocrystal anion exchange is that, in general, no workup is required to obtain pure product. Because of the volatility of these species, the exchanged halide (in the form of TMSX), as well as any residual TMSX reagent, can be fully removed after reaction by drying the nanocrystals, either *in vacuo*, with a dry nitrogen stream, or simply through passive evaporation. TMSX can also be removed by partial evacuation for nanocrystals in less volatile solvents. This feature is especially important given the poor stability of perovskite nanocrystals when exposed to many of the polar solvents commonly used in the purification of other classes of semiconductor nanocrystals: purification of perovskite nanocrystals without decomposition or degradation can be challenging, particularly if the sample must be subjected to multiple cycles of precipitation. Unlike with TMSX, nanocrystals do require such purification after anion exchange using the other reagents in our comparison.

In the course of these experiments, we have observed that complete iodide exchange on $CsPbBr_3$ nanocrystals generates $CsPbI_3$ nanocrystals whose powder XRD pattern cannot be adequately described by the cubic phase of $CsPbI_3$; Figure 4A shows representative data. Perovskite $CsPbI_3$ nanocrystals are frequently assumed to possess the cubic $Pm\bar{3}m$ crystal structure, which has been described at high temperatures in bulk. Recent detailed studies have suggested that the correct structure is an orthorhombic γ phase related to that observed in $CsPbBr_3$ nanocrystals, however.[21] The powder XRD pattern in Figure 4A can be explained by such an orthorhombic (*Pnma*) perovskite phase. In this structure, distortions of PbI_6 octahedra (resulting in Pb−I−Pb bond angles significantly below 180°) lower the crystal symmetry from cubic to orthorhombic (Figure 4B).

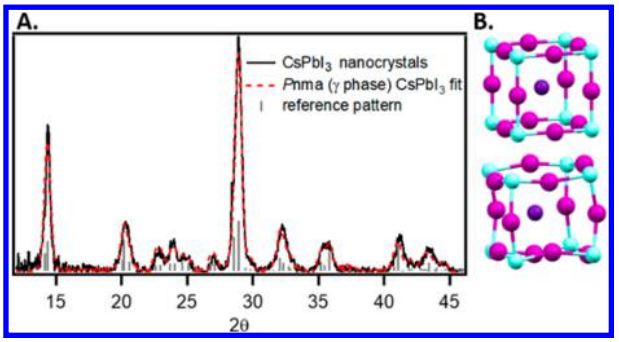

Figure 4. Identification of orthorhombic perovskite γ phase in $CsPbI_3$ nanocrystals synthesized by anion exchange. (A) Powder XRD data for $CsPbI_3$ nanocrystals (black), simulated reference pattern (gray sticks) and fit (red); see text/SI for details. (B) Unit cell of cubic perovskite $CsPbI_3$ (top) and an analogous subunit of the orthorhombic γ phase showing distortions of the PbI_6 units (bottom).

Experimental identification of this orthorhombic perovskite γ phase of $CsPbI_3$ is relatively rare. Recently, Fu et al. reported selective stabilization of the γ phase in $CsPbI_3$ thin films,[22] and Marronnier et al. have used *in situ* synchrotron XRD diffraction to study the γ phase in bulk on an undercooled sample at 325 K.[23] The likely presence of an orthorhombic perovskite γ phase in colloidal $CsPbI_3$ nanocrystals has only recently been suggested,[21,24] however, and the structure is still frequently assumed to be cubic. Figure 4A shows that the powder XRD data from our $CsPbI_3$ nanocrystals agrees well with that reported for bulk by Marronnier et al.[23] Combined with other recent reports,[21,24] our data suggest that the orthorhombic γ perovskite phase is likely widespread for $CsPbI_3$ nanocrystals, as is now well-established for $CsPbBr_3$.[25]

Considering these successes in $CsPbX_3$ nanocrystal anion exchange, we were interested in examining whether TMSX reagents could also be used on polycrystalline perovskite thin films, and in particular whether TMSI could be used to access perovskite-phase $CsPbI_3$ films that can be difficult to synthesize directly because of decomposition into the nonperovskite

DOI: 10.1021/acs.chemmater.8b02100
Chem. Mater. 2018, 30, 4887−4891

orthorhombic δ phase. Prior work on anion exchange in polycrystalline thin films of all-inorganic perovskites is limited, although Hoffman et al. have recently reported the transformation of sintered nanocrystal films of $CsPbBr_3$ to perovskite $CsPbI_3$ by anion exchange using PbI_2 solutions, and anion exchange on hybrid perovskite thin films has also been reported.[26,27]

To test this chemistry, we prepared 350 nm thick $CsPbBr_3$ films on glass substrates following a previously reported method;[28] absorption spectra and XRD analysis confirm the formation of orthorhombic $CsPbBr_3$ (Figure 5). These films were heated to 75 °C in toluene solutions of 10 vol % TMSI for 4 h under inert atmosphere. Figure 5 shows a photograph and characterization data (XRD and UV−vis absorbance) of representative films before and after this reaction. These data confirm successful anion exchange to yield $CsPbI_3$. Notably, the XRD is again most consistent with the orthorhombic perovskite γ phase, as observed for our anion-exchanged nanocrystals, suggesting that the orthorhombic cation sublattice of the starting $CsPbBr_3$ film is preserved.[29,30] The resulting $CsPbI_3$ films are stable in inert atmosphere, but decompose rapidly to the yellow nonperovskite δ phase when exposed to ambient air. At intermediate times before the $CsPbBr_3$ film is fully converted to $CsPbI_3$, we observe absorption and XRD features consistent with inhomogeneous exchange creating regions with different $CsPbBr_{3x}I_{3(1-x)}$ compositions, similar to what was observed by Hoffman et al. for thick films.[26]

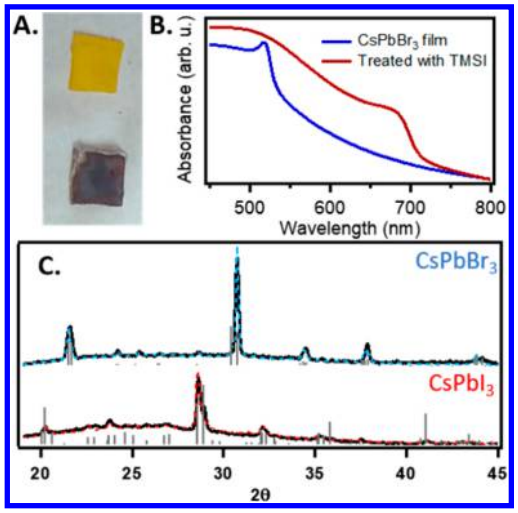

Figure 5. (A) Photograph of a $CsPbBr_3$ film (top) and a sample treated with TMSI. (B) Absorbance spectra of film before and after treatment with TMSI. (C) Powder XRD diffraction patterns for $CsPbBr_3$ film and the same film after treatment with TMSI. Data (black) is overlaid (dotted lines, blue and red) with simulated patterns of orthorhombic perovskite structures.

In conclusion, trimethylsilyl halide reagents excel for anion exchange (Cl^- to Br^-, or Br^- to I^-) in $CsPbX_3$ nanocrystals. Their key advantages include strong thermodynamic driving forces for incorporation of heavier halides, their volatility (which precludes the need for any workup), and their inertness toward undesired side reactions or nanocrystal decomposition. Through quantitative studies, we have demonstrated that the highly favorable formation of stronger Si−Br or Si−Cl bonds allows nearly stoichiometric anion exchange with these reagents. We have further demonstrated that TMSI can be used to convert polycrystalline thin films of bulk perovskite $CsPbBr_3$ into $CsPbI_3$ by anion exchange. With these advantages, TMSX reagents should find widespread use in the synthesis and study of all classes of metal-halide nanocrystals.

■ ASSOCIATED CONTENT

Supporting Information

The Supporting Information is available free of charge on the ACS Publications website at DOI: 10.1021/acs.chemmater.8b02100.

Experimental methods, additional materials characterization, and anion-exchange data (PDF)

■ AUTHOR INFORMATION

Corresponding Author

*D. R. Gamelin. E-mail: gamelin@chem.washington.edu.

ORCID

Sidney E. Creutz: 0000-0003-4440-5336

Daniel R. Gamelin: 0000-0003-2888-9916

Notes

The authors declare no competing financial interest.

■ ACKNOWLEDGMENTS

This research was partially supported by the U.S. National Science Foundation (NSF) through DMR-1505901 and DMR-1807394 to D.R.G. Part of this work was conducted at the Molecular Analysis Facility, a National Nanotechnology Coordinated Infrastructure site at UW that is supported in part by the NSF (grant ECC-1542101), UW, the Molecular Engineering & Sciences Institute, the Clean Energy Institute, and the National Institutes of Health. This research was supported by an appointment to the Intelligence Community Postdoctoral Research Fellowship Program at UW, administered by Oak Ridge Institute for Science and Education through an interagency agreement between the U.S. Department of Energy and the Office of the Director of National Intelligence (S.E.C.).

■ REFERENCES

(1) Protesescu, L.; Yakunin, S.; Bodnarchuk, M. I.; Krieg, F.; Caputo, R.; Hendon, C. H.; Yang, R. X.; Walsh, A.; Kovalenko, M. V. Nanocrystals of Cesium Lead Halide Perovskites ($CsPbX_3$, X = Cl, Br, and I): Novel Optoelectronic Materials Showing Bright Emission with Wide Color Gamut. *Nano Lett.* **2015**, *15*, 3692−3696.

(2) Akkerman, Q. A.; Rainò, G.; Kovalenko, M. V.; Manna, L. Genesis, challenges and opportunities for colloidal lead halide perovskite nanocrystals. *Nat. Mater.* **2018**, *17*, 394−405.

(3) Akkerman, Q. A.; D'Innocenzo, V.; Accornero, S.; Scarpellini, A.; Petrozza, A.; Prato, M.; Manna, L. Tuning the Optical Properties of Cesium Lead Halide Perovskite Nanocrystals by Anion Exchange Reactions. *J. Am. Chem. Soc.* **2015**, *137*, 10276−10281.

(4) Nedelcu, G.; Protesescu, L.; Yakunin, S.; Bodnarchuk, M. I.; Grotevent, M. J.; Kovalenko, M. V. Fast Anion-Exchange in Highly Luminescent Nanocrystals of Cesium Lead Halide Perovskites ($CsPbX_3$, X = Cl, Br, I). *Nano Lett.* **2015**, *15*, 5635−5640.

(5) Jang, D. M.; Park, K.; Kim, D. H.; Park, J.; Shojaei, F.; Kang, H. S.; Ahn, J.-P.; Lee, J. W.; Song, J. K. Reversible Halide Exchange Reaction of Organometal Trihalide Perovskite Colloidal Nanocrystals for Full-Range Band Gap Tuning. *Nano Lett.* **2015**, *15*, 5191−5199.

(6) Leng, M.; Chen, Z.; Yang, Y.; Li, Z.; Zeng, K.; Li, K.; Niu, G.; He, Y.; Zhou, Q.; Tang, J. Lead-Free, Blue Emitting Bismuth Halide

DOI: 10.1021/acs.chemmater.8b02100
Chem. Mater. 2018, 30, 4887−4891

Perovskite Quantum Dots. *Angew. Chem., Int. Ed.* **2016**, *55*, 15012−15016.
(7) Creutz, S. E.; Crites, E. N.; De Siena, M. C.; Gamelin, D. R. Colloidal Nanocrystals of Lead-Free Double-Perovskite (Elpasolite) Semiconductors: Synthesis and Anion Exchange To Access New Materials. *Nano Lett.* **2018**, *18*, 1118−1123.
(8) Zhang, J.; Yang, Y.; Deng, H.; Farooq, U.; Yang, X.; Khan, J.; Tang, J.; Song, H. High Quantum Yield Blue Emission from Lead-Free Inorganic Antimony Halide Perovskite Colloidal Quantum Dots. *ACS Nano* **2017**, *11*, 9294−9302.
(9) Udayabhaskararao, T.; Houben, L.; Cohen, H.; Menahem, M.; Pinkas, I.; Avram, L.; Wolf, T.; Teitelboim, A.; Leskes, M.; Yaffe, O.; Oron, D.; Kazes, M. A Mechanistic Study of Phase Transformation in Perovskite Nanocrystals Driven by Ligand Passivation. *Chem. Mater.* **2018**, *30*, 84−93.
(10) Balakrishnan, S. K.; Kamat, P. V. Ligand Assisted Transformation of Cubic $CsPbBr_3$ Nanocrystals into Two-Dimensional $CsPb_2Br_5$ Nanosheets. *Chem. Mater.* **2018**, *30*, 74−78.
(11) Liu, W.; Lin, Q.; Li, H.; Wu, K.; Robel, I.; Pietryga, J. M.; Klimov, V. I. Mn^{2+}-Doped Lead Halide Perovskite Nanocrystals with Dual-Color Emission Controlled by Halide Content. *J. Am. Chem. Soc.* **2016**, *138*, 14954−14961.
(12) Milstein, T.; Kroupa, D.; Gamelin, D. R. Picosecond Quantum Cutting Generates Photoluminescence Quantum Yields over 100% in Ytterbium-Doped $CsPbCl_3$ Nanocrystals. *Nano Lett.* **2018**, *18*, 3792−3799.
(13) Jung, M. E.; Martinelli, M. J.; Olah, G. A.; Prakash, G. K. S.; Hu, J. Iodotrimethylsilane. In *Encyclopedia of Reagents for Organic Synthesis*; John Wiley & Sons, 2005.
(14) Martinelli, M. J.; Pollack, S. R. Bromotrimethylsilane. In *Encyclopedia of Reagents for Organic Synthesis*; John Wiley & Sons, 2006.
(15) Leahy, E. M.; Zhang, W. Chlorotrimethylsilane. In *Encyclopedia of Reagents for Organic Synthesis*; John Wiley & Sons, 2008.
(16) Walsh, R. Bond dissociation energy values in silicon-containing compounds and some of their implications. *Acc. Chem. Res.* **1981**, *14*, 246−252.
(17) Imran, M.; Caligiuri, V.; Wang, M.; Goldoni, L.; Prato, M.; Krahne, R.; De Trizio, L.; Manna, L. Benzoyl Halides as Alternative Precursors for the Colloidal Synthesis of Lead-Based Halide Perovskite Nanocrystals. *J. Am. Chem. Soc.* **2018**, *140*, 2656−2664.
(18) Koscher, B. A.; Bronstein, N. D.; Olshansky, J. H.; Bekenstein, Y.; Alivisatos, A. P. Surface- vs Diffusion-Limited Mechanisms of Anion Exchange in $CsPbBr_3$ Nanocrystal Cubes Revealed through Kinetic Studies. *J. Am. Chem. Soc.* **2016**, *138*, 12065−12068.
(19) De Roo, J.; Ibáñez, M.; Geiregat, P.; Nedelcu, G.; Walravens, W.; Maes, J.; Martins, J. C.; Van Driessche, I.; Kovalenko, M. V.; Hens, Z. Highly Dynamic Ligand Binding and Light Absorption Coefficient of Cesium Lead Bromide Perovskite Nanocrystals. *ACS Nano* **2016**, *10*, 2071−2081.
(20) Ravi, V. K.; Santra, P. K.; Joshi, N.; Chugh, J.; Singh, S. K.; Rensmo, H.; Ghosh, P.; Nag, A. Origin of the Substitution Mechanism for the Binding of Organic Ligands on the Surface of $CsPbBr_3$ Perovskite Nanocubes. *J. Phys. Chem. Lett.* **2017**, *8*, 4988−4944.
(21) Bertolotti, F.; Protesescu, L.; Kovalenko, M. V.; Yakunin, S.; Cervellino, A.; Billinge, S. J. L.; Terban, M. W.; Pedersen, J. S.; Masciocchi, N.; Guagliardi, A. Coherent Nanotwins and Dynamic Disorder in Cesium Lead Halide Perovskite Nanocrystals. *ACS Nano* **2017**, *11*, 3819−3831.
(22) Fu, Y.; Rea, M. T.; Chen, J.; Morrow, D. J.; Hautzinger, M. P.; Zhao, Y.; Pan, D.; Manger, L. H.; Wright, J. C.; Goldsmith, R. H.; Jin, S. Selective Stabilization and Photophysical Properties of Metastable Perovskite Polymorphs of $CsPbI_3$ in Thin Films. *Chem. Mater.* **2017**, *29*, 8385−8394.
(23) Marronnier, A.; Roma, G.; Boyer-Richard, S.; Pedesseau, L.; Jancu, J.-M.; Bonnassieux, Y.; Katan, C.; Stoumpos, C. C.; Kanatzidis, M. G.; Even, J. Anharmonicity and Disorder in the Black Phases of Cesium Lead Iodide Used for Stable Inorganic Perovskite Solar Cells. *ACS Nano* **2018**, *12*, 3477−3486.
(24) Beimborn, J. C.; Hall, L. M. G.; Tongying, P.; Dukovic, G.; Weber, J. M. Pressure Response of Photoluminescence in Cesium Lead Iodide Perovskite Nanocrystals. *J. Phys. Chem. C* **2018**, *122*, 11024−11030.
(25) Cottingham, P.; Brutchey, R. L. On the crystal structure of colloidally prepared $CsPbBr_3$ quantum dots. *Chem. Commun.* **2016**, *52*, 5246−5249.
(26) Hoffman, J. B.; Schleper, A. L.; Kamat, P. V. Transformation of Sintered CsPbBr3 Nanocrystals to Cubic $CsPbI_3$ and Gradient $CsPbBr_xI_{3-x}$ through Halide Exchange. *J. Am. Chem. Soc.* **2016**, *138*, 8603−8611.
(27) Li, G.; Ho, J. Y.-L.; Wong, M.; Kwok, H. S. Reversible Anion Exchange Reaction in Solid Halide Perovskites and Its Implication in Photovoltaics. *J. Phys. Chem. C* **2015**, *119*, 26883−26888.
(28) Kulbak, M.; Cahen, D.; Hodes, G. How Important Is the Organic Part of Lead Halide Perovskite Photovoltaic Cells? Efficient $CsPbBr_3$ Cells. *J. Phys. Chem. Lett.* **2015**, *6*, 2452−2456.
(29) De Trizio, L.; Manna, L. Forging Colloidal Nanostructures via Cation Exchange Reactions. *Chem. Rev.* **2016**, *116*, 10852−10887.
(30) Agarwal, R.; Krook, N. M.; Ren, M.-L.; Tan, L. Z.; Liu, W.; Rappe, A. M.; Agarwal, R. Anion Exchange in II−VI Semiconducting Nanostructures via Atomic Templating. *Nano Lett.* **2018**, *18*, 1620−1627.

DOI: 10.1021/acs.chemmater.8b02100
Chem. Mater. 2018, 30, 4887−4891